RESEARCH ARTICLE

Open Access

Synthesis of visible light active doped TiO$_2$ for the degradation of organic pollutants—methylene blue and glyphosate

Khalid Umar[1,5,6], Azmi Aris[1,5*], Hilal Ahmad[3], Tabassum Parveen[4], Jafariah Jaafar[2], Zaiton Abdul Majid[2], A. Vijaya Bhaskar Reddy[2] and Juhaizah Talib[1,5]

Abstract

Background: A simple hydrothermal process was applied to synthesize the doped TiO$_2$ particles with different concentrations as well as different metal ions (Mn, Ce and La).

Methods: The synthesis of Mn-doped-TiO$_2$ nanoparticles was done by using a hydrothermal method from hydrolysis of titanium tetrachloride in aqueous solution. The photocatalytic activities were checked by studying the degradation of two model organic pollutants.

Results: The material was characterized by X-ray diffraction, scanning electron microscopy, and UV–Visible spectroscopy. The X-ray diffraction pattern studied for doped TiO$_2$ particles suggests the anatase phase with a crystalline nature. Doped TiO$_2$ particles showed a porous and complex nature with a highly rough surface. The photocatalytic activity of Mn- Ce- and La-doped TiO$_2$ with different metal-ion concentrations of 0.15-0.60% show that the degradation rate of all of the pollutants increases with an increase in the dopant concentration from 0.15 to 0.45%, and a further increase in the dopant concentration decreased the degradation rate.

Conclusions: The results indicate that TiO2 with a concentration of 0.45% for all metal ions (Mn, Ce and La) shows the highest activity. Among studied dopent TiO2 with Mn (0.45%) showed the best degradation activity.

Keywords: Doped TiO$_2$, Photocatalytic degradation, Pesticide, Dye, Visible light

Background

During the past three decades, photocatalytic processes that involve semiconductor particles irradiated by UV light have been shown to be potentially beneficial in the degradation of various types of pollutants in aqueous suspensions (Blake 2001; Neppolian et al. 2002; Chaleshtori et al. 2013; Geng et al. 2009; Kim et al. 2016; Zhang et al. 2015; Han et al. 2016; Liu et al. 2016; Yang and Xu 2016; Umar et al. 2013a; Akpan and Hameed 2009; Lv et al. 2009; Arslan et al. 2002; Umar et al. 2015). Several metal

chalcogenides (ZnS, CdS, CdSe) and metal oxides (ZrO$_2$, TiO$_2$, ZnO, SnO$_2$) have been extensively used for the degradation of a variety of pollutants. Among these semiconductors, TiO$_2$ is the most widely used oxide because it is chemically and biologically inert, photo catalytically stable, resistant to strong acids and bases, and stable under illumination (Fox and Dulay 1993). According to the estimated valence band (VB) and conduction band (CB) energies of TiO$_2$, the band gap energy is found to be 3.2 eV. Therefore, it can only be performed its activity by UV light due to its large band gap energy. Recently, doping of TiO$_2$ with metals and non-metals has received great attention because it can shift the photocatalytic response of catalysts from the UV region to the visible-light region and ultimately can harvest solar energy (Umar et al. 2013b; Colon et al. 2006; Fan et al. 2010; Zhang and Zhu

* Correspondence: azmi.aris@utm.my
[1]Department of Environmental Engineering, Faculty of Civil Engineering, Universiti Teknologi Malaysia, 81310 Johor Bahru, Johor, Malaysia
[5]Centre for Environmental Sustainability and Water Security (IPASA), Research Institute for Sustainable Environment, Universiti Teknologi Malaysia, 81310 Johor Bahru, Johor, Malaysia
Full list of author information is available at the end of the article

Umar *et al. Journal of Analytical Science and Technology* (2016) 7:29

Page 2 of 8

2012; Liu et al. 2009; Binas et al. 2012; Uhm et al. 2006). Up to date, there are some studies reported in the literature on the doping of TiO_2 by various routes and their photocatalytic performance for the degradation of various types of pollutants (Stengl and Bakardjieva 2010; Devi and Murthy 2008; Devi et al. 2009a; Papadimitriou et al. 2011; Jin et al. 2008; Peng et al. 2005; Stengl et al. 2009; Liqiang et al. 2004; Chen et al. 2011). In brief, Rashad et al. (2013) prepared TiO_2 nanoparticles doped with (Co and Mn) by hydrothermal technique and checked their performance on degradation of methylene blue (MB) under UV light. The decomposition of phenol in the presence of Mn-doped TiO_2 have been reported by Paul et al. (2014). Recently, Rangel-Vázqueza et al. (2015) prepared the Sn-doped TiO_2 using sol gel method and tested its activity for the degradation of 2,4-dichlorophenoxya-cetic acid. On the other hand, Kuyumcu et al. (2015) synthesizes the doped TiO_2 using different metal ions and degradation of two dyes under visible light has also been reported.

Dyes and pesticides have been used by mankind for many decades for different useful purposes. However, their existence in water bodies at this time has become a challenge for researchers and environmental authorities because these pollutants create some serious problems to the surrounding ecosystems and causes human health disorders. The worldwide annual production of dyes increases day by day, a prominent portion of which is vanished during the dyeing process in various types of industries, which finally pollutes our aquatic environment (Ajit et al. 2006; Kolpin et al. 2002; Umar et al. 2012). Furthermore, many pesticides have been detected in both surface and ground water in different localities worldwide (Knee et al. 2010; STORET water quality file 1988; Rovedatti et al. 2001). This polluted water is not useful for irrigation or domestic purposes. Therefore, these pollutants must be eliminated from water bodies before they can be used.

The objective of this study was to fabricate visible-light-responsive photo catalyst using different concentrations of dopent using a simple hydrothermal process. The paper also addresses the enhanced photocatalytic activities of metal-doped TiO_2 for the degradation of organic compounds, such as methylene blue (dye) and gly-phosate (pesticide).

Methods
Preparation and characterization
The synthesis of Mn-doped-TiO_2 nanoparticles was done by using a hydrothermal method from hydrolysis of titanium tetrachloride in aqueous solution. In a typical synthesis, 1.6 mL of titanium tetrachloride was added dropwise into 30 mL of deionized water under stirring at room temperature to obtain solution 1. The

calculated amount of manganese (II) sulfate monohy-drate (0.15–0.60%) were dissolved to 15 mL of deionized water at room temperature to form solution 2. The above solutions 1 and 2 were mixed and stirred for 15 min. The resulting mixture was transferred into a 50-mL stainless steel autoclave and heated at 140 °C for 5 h. The obtained precipitate was washed with distilled water and then dried at 110 °C for 10 h in an oven. For Ce- and La-doped and undoped TiO_2, the procedure was the same except the difference in dopants.

The samples of undoped and doped TiO_2 particles were analyzed by XRD using Bruker AXS D8 Advance over the range of 20 to 80 kV with Cu Kα radiations (λ = 1.5418 Å), which was operated at 4°/min scanning rate with a voltage of 30 kV and a current of 15 mA. The Shimadzu UV–vis spectrophotometer (Model 1601) was used to record the UV–vis spectra in the range of 300–800 nm. Using SEM (LEO, 435 VF) at different magnifications, WD 15 mm, the prepared material was examined for structural morphology.
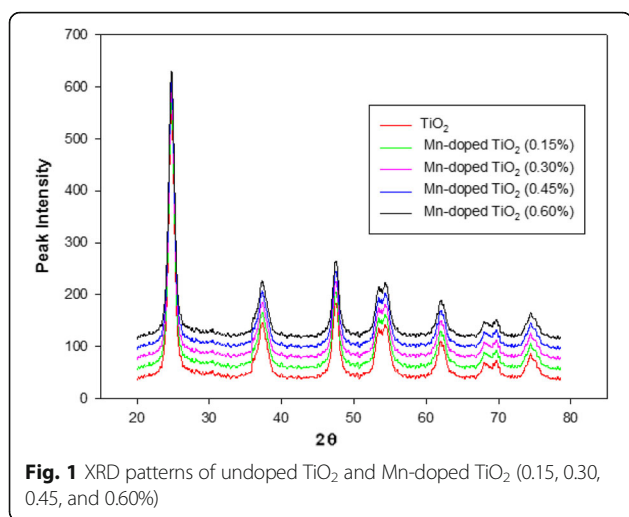
Photocatalytic reactions
Stock solution of organic pollutants, methylene blue (dye), and glyphosate (pesticide) containing desired concentrations were prepared in double-distilled water. An immersion well photochemical reactor made of Pyrex glass equipped with a magnetic stirring bar, water circulating jacket, and an opening for supply of atmospheric oxygen was used. An aqueous solution (250 mL) of the organic pollutants was poured into the photoreactor. Then, required amount of photocatalyst was added to conduct irradiation process. The solution was stirred and bubbled with atmospheric oxygen for at least 10 min, prior to illumination in order to allow equilibration of the system. The visible-light halogen linear lamp (500 W, 9500 Lumens) was used to conduct irradiation experiments. The samples (8 mL) were collected before and at regular intervals during the irradiation, and the analysis were done after removal of photocatalyst using centrifugation.

Results and discussion
Catalysts characterization
The XRD patterns of the synthesized undoped and doped TiO_2 with different concentrations of Mn, Ce, and La were analyzed. Figure 1 shows the XRD pattern of undoped and Mn-doped TiO_2 as a representative example. The peaks obtained after the sample analysis, which correspond to the (101), (103), (004), (112), (200), (105), (211), (118), (116), and (220) crystal planes, are well indexed to the standard pattern of the anatase phase and also exhibit the crystalline nature of undoped and doped TiO_2. The XRD patterns of the undoped and doped TiO_2 show no significant changes. Note that the

Umar et al. Journal of Analytical Science and Technology (2016) 7:29

Page 3 of 8

Fig. 1 XRD patterns of undoped TiO$_2$ and Mn-doped TiO$_2$ (0.15, 0.30, 0.45, and 0.60%)

XRD patterns do not display any peak that corresponds to the dopant possibly because the sample contains a lower concentration of the dopant than the TiO$_2$ concentration. Furthermore, Mn^{2+} (0.080 Å) and La^{3+} (0.1016 Å) have larger ionic radii than Ti^{4+} (0.068 Å). Therefore, it is difficult for these dopants to act as interstitial impurities, so they may be present on the surface layer of TiO$_2$ (Peng et al. 2005; Devi et al. 2009b).

Using the Debye Scherer formula, the average anatase crystallite size of doped and undoped TiO$_2$ nanoparticles was determined (Eq. 1).

$$D = \frac{K\lambda}{\beta \cos\theta} \tag{1}$$

where D = crystallite size, K = shape factor, λ = wavelength, β = full width at half maximum, and θ = diffraction angle. The mean sizes of the crystallites of undoped and doped samples are shown in Table 1. The crystallite size decreases with an increase in the dopant concentration possibly because of possible formation of metal–oxygen–titanium bonds, which inhibits the size of crystal grains (Devi et al. 2009a).

When UV–vis light excites, it generates electrons and holes in the band structure (or molecular energy levels) of the material. Thus, the UV–vis absorption spectra of
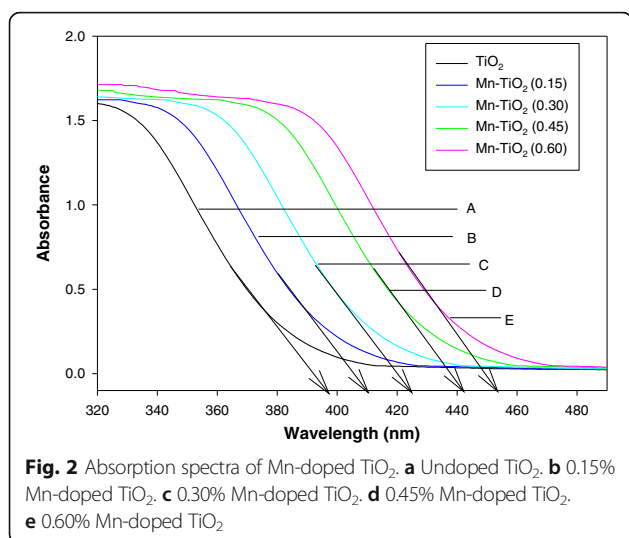
undoped TiO$_2$ and doped TiO$_2$ with varying concentrations of Mn and La (dopant) were studied, and a representative example, which is the UV–vis absorption spectra of undoped and Mn-doped TiO$_2$, is shown in Fig. 2. At the obtained wavelength from the UV–vis absorption spectra, the band gap energies of undoped and doped TiO$_2$ particles width were calculated using Eq. 2 and are listed in Table 2.

$$\text{Band energy (eV)} = 1240/\text{wavelength(nm)} \tag{2}$$

The UV–vis absorption spectra of Mn-doped TiO$_2$ show a red shift in the band-gap transition possibly because the metal doping introduces new energy levels in the band gap of TiO$_2$, which decreases the band gap energy (Devi et al. 2009b). In addition, the reduction in band gap of TiO$_2$ may be led by the overlapping of d-orbital (dopant ions) with the conduction band of TiO$_2$ and thus, resulting in the absorption of light in visible region (Raza et al). The structural characterization of undoped and doped TiO$_2$ was performed using SEM. The surface morphology of undoped and doped TiO$_2$ particles with metal ions (0.45%) is shown in Fig. 3. The SEM image of undoped TiO$_2$ exhibits a sponge-like network with high roughness whereas the doped TiO$_2$ particles show a porous and complex nature with a highly rough surface, which results in a high surface area of 472 m^2/g estimated by using the multi-point Brunauer–Emmett–Teller (BET) theory after the adsorption and desorption of nitrogen gas. The photoluminescence (PL) spectra are depicted in Fig. 4, which are used to investigate the activity of a photocatalyst, which is depending upon the rate of the recombination of electrons and holes. The energy dissipated by the electron–hole recombination is directly proportional to the recombination rate. The trend based on fluorescence intensity of these samples follow the order: pure TiO$_2$ > Mn-doped TiO$_2$ (0.15%) > Mn-doped TiO$_2$ (0.30%) > Mn-doped TiO$_2$ (0.60%) > Mn-doped TiO$_2$ (0.45%). It suggests that TiO$_2$ doped with up to the amount of dopant (Mn, 0.45%) decrease the rate of recombination rate. With further increase in dopant (Mn, 0.60%) content, the peak intensity increases

Table 1 Crystallite size of undoped and doped-TiO$_2$ with different concentration of Mn, Ce and La

S.No.	Dopant concentration (%)	Dopant/crystallite size (nm)	Dopant/crystallite size (nm)	Dopant/crystallite size (nm)
1	0	None/15.4	None/15.4	None/15.4
2	0.15	Mn/12.9	Ce/13.0	La/13.2
3	0.30	Mn/10.6	Ce /10.7	La/10.8
4	0.45	Mn/9.1	Ce / 9.2	La/ 9.3
5	0.60	Mn/7.9	Ce / 8.0	La/ 8.1

Fig. 2 Absorption spectra of Mn-doped TiO$_2$. **a** Undoped TiO$_2$. **b** 0.15% Mn-doped TiO$_2$. **c** 0.30% Mn-doped TiO$_2$. **d** 0.45% Mn-doped TiO$_2$. **e** 0.60% Mn-doped TiO$_2$

which indicate the rate of recombination are faster. The reason for this may be attributed to inefficient diffusion of Mn into TiO$_2$ lattice and subsequent decrease in band gap. Therefore, the doping quantity (Mn, 0.45%) can prove as an optimum dopant concentration in this case.

The photodegradation of organic pollutants methylene blue (dye) and glyphosate (pesticide) was monitored by measuring the absorbance at their λ_{max} as a function of the irradiation time using the UV spectroscopic analysis technique (Shimadzu UV–vis 1601). The concentrations of organic pollutants were calculated based on the standard calibration curve, which was obtained from the individual absorbance of these compounds at different known concentrations.

Photocatalytic activity
Photocatalysis of methylene blue in presence of Mn-doped TiO$_2$
An aqueous solution of methylene blue (0.50 mM, 250 mL) was irradiated with a visible light halogen lamp in the presence of Mn-doped TiO$_2$ (1 g/L) with constant stirring and bubbling of atmospheric oxygen. The decolorization of the dye was monitored by measuring the change in absorbance as a function irradiation time. As a representative example, Fig. 5 shows the change in

concentration of the dye as a function of irradiation time in the presence (0.45% Mn-doped) and absence of Mn-doped TiO$_2$. It could be seen from the figure that 75% decolorization of methylene blue take place after 300 min of irradiation in the presence of Mn-doped TiO$_2$ and atmospheric oxygen. On the other hand, in the absence of photocatalyst, no observable decrease in the dye concentration could be seen.

Photocatalysis of glyphosate in presence of Mn-doped TiO$_2$
An aqueous solution of glyphosate (0.035 mM, 250 mL) was irradiated in the presence of Mn-doped TiO$_2$ under analogous conditions. As a representative example, Fig. 6 shows the change in concentration of glyphosate in the presence (0.45% Mn-doped) and absence of Mn-doped TiO$_2$ as a function of irradiation time. In this pesticide derivative, 80% destruction takes place after 300 min of irradiation in the presence of Mn-doped TiO$_2$ whereas in the absence of photocatalyst, no observable decrease in the pesticide concentration could be seen.

The curve of the change in concentration as a function of the irradiation time in the presence of metal-doped TiO$_2$ for methylene blue and glyphosate (shown in Figs. 5 and 6) can be fitted reasonably well by an exponential decay curve, which suggests pseudo first-order kinetics. Figure 7 shows the linear regression curve fit for the natural logarithm of concentration vs. irradiation time for the degradation of methylene blue. For each experiment, the rate constant was calculated from the plot of the natural logarithm of the concentration as a function of the irradiation time. The degradation rate was calculated using Eq. (3);

$$-d[C]/dt = kC^n \qquad (3)$$

where C = concentration of the pollutant, k = rate constant, and n = order of reaction.
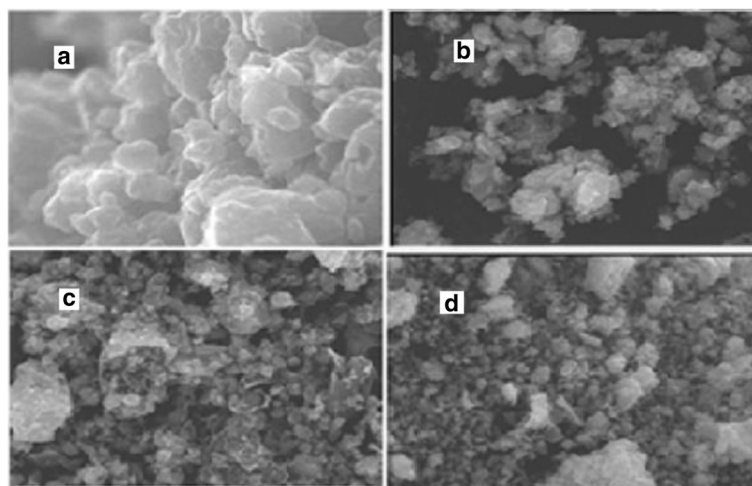
The degradation rate was calculated in terms of moles per liter per minute.

Photocatalytic activity of Mn-, Ce-, and La-doped TiO$_2$ for the degradation of organic pollutants
The photocatalytic activity of Mn-, Ce-, and La-doped TiO$_2$ with different metal-ion concentrations of 0.15–0.60% was tested by studying the degradation

Table 2 Band gap energy of undoped and doped-TiO$_2$ with different concentration of Mn, Ce and La

S.No.	Dopant concentration (%)	Dopant/ Band gap (eV)	Dopant/Band gap (eV)	Dopant/Band ap (eV)
1	0	None/3.18	None/3.18	None/3.18
2	0.15	Mn/2.98	Ce/2.99	La/3.00
3	0.30	Mn/2.88	Ce /2.90	La/2.93
4	0.45	Mn/2.78	Ce/2.81	La/2.83
5	0.60	Mn/2.72	Ce /2.74	La/2.76

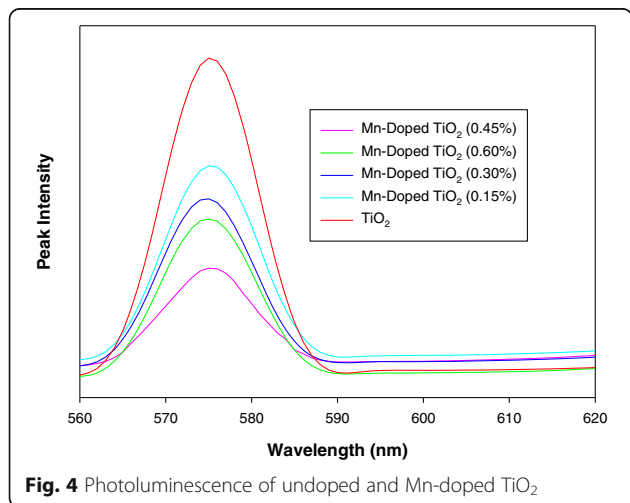Umar *et al. Journal of Analytical Science and Technology* (2016) 7:29

Page 5 of 8

Fig. 3 SEM images of undoped and doped TiO_2. **a** undoped TiO_2. **b** 0.45% Mn-doped TiO_2. **c** 0.45% Ce-doped TiO_2. **d** 0.45% La-doped TiO_2
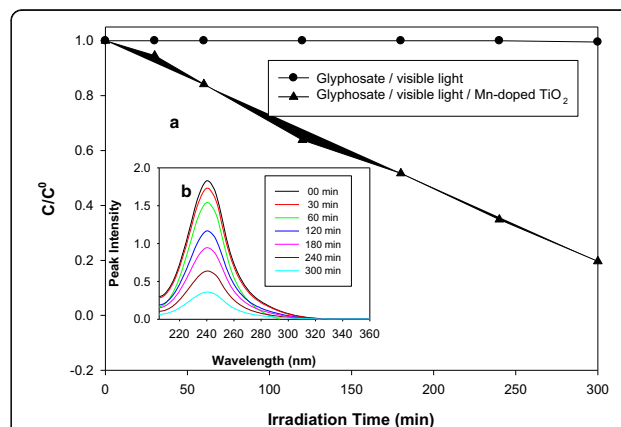
of two different categories of organic pollutants such as methylene blue (dye) and glyphosate (pesticide), in aqueous suspension under visible light in atmospheric oxygen. Figures 7, 8, and 9 show the degradation rate of two organic pollutants in the presence of undoped (pure TiO_2) and doped TiO_2 (Mn, Ce, and La, 0.15–0.60%). The results show that the degradation rate of all of the pollutants increases with an increase in the dopant concentration from 0.15 to 0.45%, and a further increase in the dopant concentration decreased the degradation rate.

In this study, the optimal dosage of metal ions for the degradation of both pollutants is 0.45%, after which the degradation rate decreases. The increase in the photocatalytic activity by increasing the dopant concentration can be attributed to the higher surface barrier and narrower
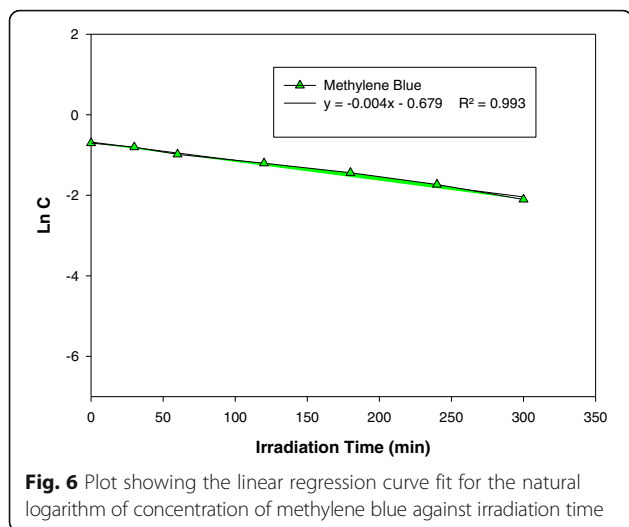
space charge region when the content of doping ions increases. The electron–hole pairs in the region are efficiently separated; as a result, recombination slows down and the electron–hole pairs are readily available (Stengl et al. 2009). However, after reaching the optimal condition when the doping content is increased, the space charge region becomes notably narrow, and the penetration depth of light into TiO_2 greatly exceeds the space charge layer. Therefore, the recombination of the photo-generated electron–hole pairs becomes easier, and fewer charge carriers reach the surface to initiate the degradation phenomenon, which decrease the photocatalytic activity (Stengl et al.

Fig. 4 Photoluminescence of undoped and Mn-doped TiO_2
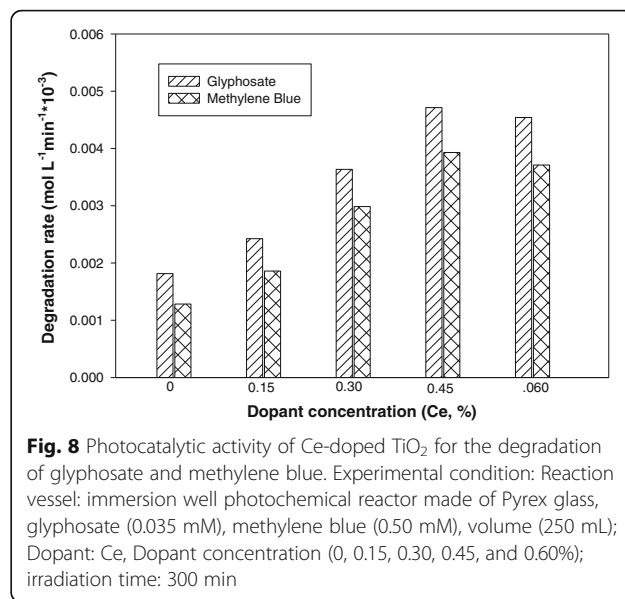

Fig. 5 a Change in concentration as a function of time on irradiation of an aqueous solution of glyphosate in the absence and presence of Mn-doped TiO_2. **b** Change in absorbance as a function of irradiation time in the presence of photocatalyst. Experimental conditions: Reaction vessel: immersion well photochemical reactor made of Pyrex glass, glyphosate (0.035 mM), volume (250 mL); Dopant: Mn, Dopant concentration (0.45%); irradiation time: 300 min
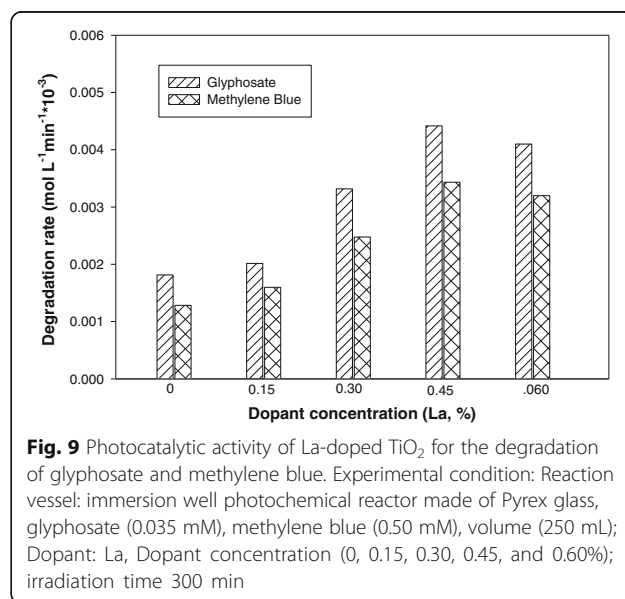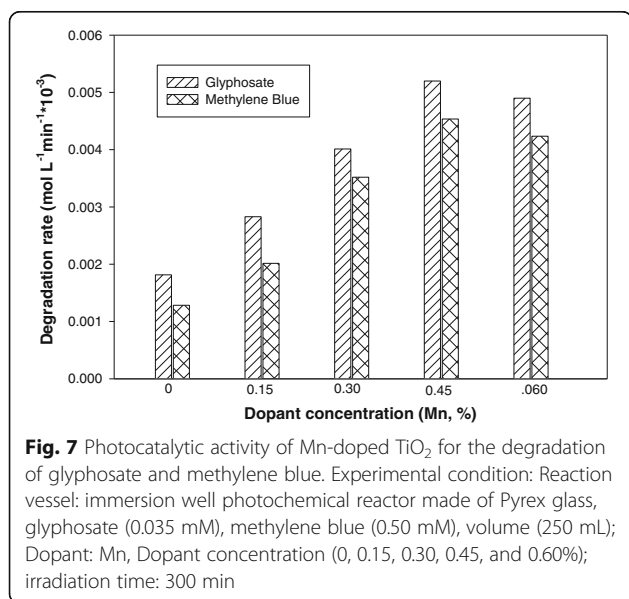
Umar et al. Journal of Analytical Science and Technology (2016) 7:29

Page 6 of 8

Fig. 6 Plot showing the linear regression curve fit for the natural logarithm of concentration of methylene blue against irradiation time

Fig. 8 Photocatalytic activity of Ce-doped TiO_2 for the degradation of glyphosate and methylene blue. Experimental condition: Reaction vessel: immersion well photochemical reactor made of Pyrex glass, glyphosate (0.035 mM), methylene blue (0.50 mM), volume (250 mL); Dopant: Ce, Dopant concentration (0, 0.15, 0.30, 0.45, and 0.60%); irradiation time: 300 min

2009). The doping mechanism of Mn in titanium dioxide is shown in Fig. 10.

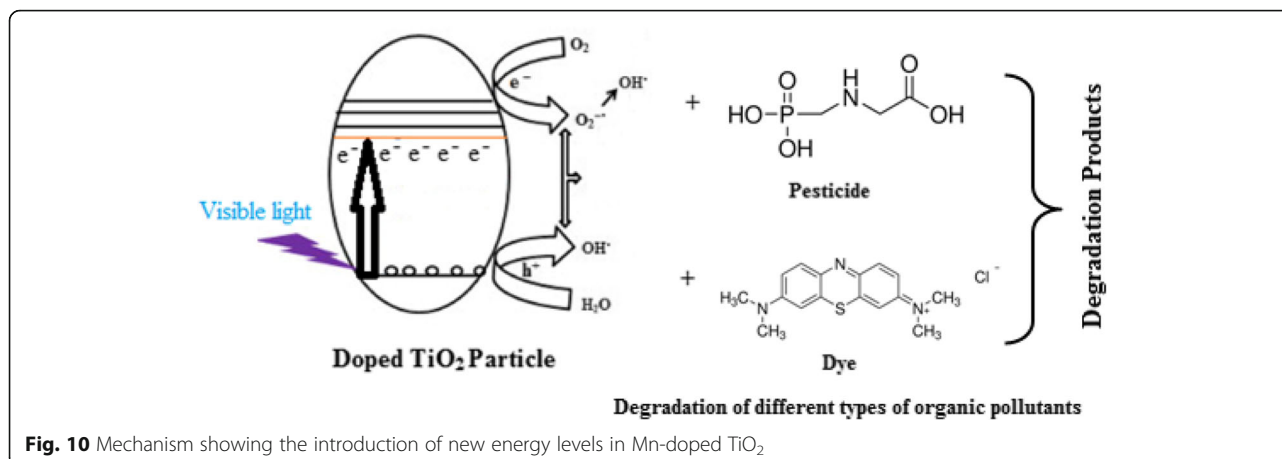## Photodegradation of methylene blue and glyphosate in presence of different photocatalysts

To observe the effect of different photocatalysts on the degradation of two types of pollutants, the degradation of these compounds was studied in the presence of PC 500, ZnO, and metal-doped TiO_2 (0.45% Mn, Ce, and La) under an analogous condition. Figure 11 shows the degradation pattern of these compounds in the presence of different types of photocatalyts. The result indicates that 0.45% Mn-doped TiO_2 is better than the other photocatalyts for the degradation of both the compounds. The better activity of Mn-doped TiO_2 as

compared to other photocatalysts for the degradation of organic pollutants can be understood by considering the fact that it (Mn^{2+}) has unique half-filled electronic structure. The trapping of electron by Mn^{2+} is temporary, and it has stable d^5 configuration. Thus, it can easily transfer the trapped electron to reacting species which can participate in the reaction and ultimately enhance the photocatalytic activity (Zhu et al. 2006). Moreover, when the ion catches an electron or a hole, the half-filled electronic configuration is disturbed; to restore its original position, the trapped electron or hole is transferred, which helps to generate hydroxyl and superoxide radicals (Devi et al. 2009a).
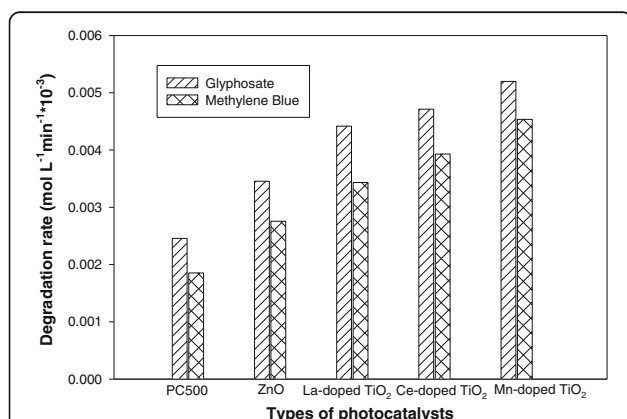

Fig. 7 Photocatalytic activity of Mn-doped TiO_2 for the degradation of glyphosate and methylene blue. Experimental condition: Reaction vessel: immersion well photochemical reactor made of Pyrex glass, glyphosate (0.035 mM), methylene blue (0.50 mM), volume (250 mL); Dopant: Mn, Dopant concentration (0, 0.15, 0.30, 0.45, and 0.60%); irradiation time: 300 min

Fig. 9 Photocatalytic activity of La-doped TiO_2 for the degradation of glyphosate and methylene blue. Experimental condition: Reaction vessel: immersion well photochemical reactor made of Pyrex glass, glyphosate (0.035 mM), methylene blue (0.50 mM), volume (250 mL); Dopant: La, Dopant concentration (0, 0.15, 0.30, 0.45, and 0.60%); irradiation time 300 min

Umar *et al. Journal of Analytical Science and Technology* (2016) 7:29

Page 7 of 8

Fig. 10 Mechanism showing the introduction of new energy levels in Mn-doped TiO_2

Conclusions

TiO_2 particles were doped with different concentrations of Mn and La (0.15–0.60%), and their photocatalytic activity was tested by studying the degradation of methylene blue and glyphosate as organic pollutants. The anatase phase with crystalline nature is shown in the XRD analysis. The SEM image of undoped TiO_2 exhibits a sponge-like network of high roughness, whereas the doped TiO_2 particles show a porous and complex nature with a highly rough surface. The photocatalytic results show that TiO_2 with a dopant concentration of 0.45% for both the metal ions has the highest photocatalytic performance using visible light. Among the photocatalysts, the Mn-doped TiO_2 (0.45%) photocatalyst shows a better degradation rate than the other photocatalysts.

Fig. 11 Degradation rate of glyphosate and methylene blue in the presence of different photocatalysts. Experimental condition: Reaction vessel: immersion well photochemical reactor made of Pyrex glass, glyphosate (0.35 mM), methylene blue (0.50 mM), volume (250 mL); photocatalysts: PC500 (1 g/L), ZnO (1 g/L), 0.45% La-doped TiO_2 (1 g/L), 0.45% Ce-doped TiO_2 (1 g/L), and 0.45% La-doped TiO_2 (1 g/L); irradiation time: 300 min

Authors' contributions
AA and KU designed the experiments. KU and HA carried out the synthesis and characterization. JJ and ZAM edited the manuscript. The rest of the authors performed the experiments and wrote their experimental section. Moreover, KU and HA revised the whole manuscript and resubmitted after due revision. All authors read and approved the final manuscript.

Competing interests
The authors declare that they have no competing interests.

Author details
[1]Department of Environmental Engineering, Faculty of Civil Engineering, Universiti Teknologi Malaysia, 81310 Johor Bahru, Johor, Malaysia. [2]Department of Chemistry, Faculty of Science, Universiti Teknologi Malaysia, 81310 Johor Bahru, Johor, Malaysia. [3]Centre for Nanoscience and Nanotechnology, Jamia Millia Islamia, New Delhi, India. [4]Department of Civil Engineering, Indian Institute of Technology, Roorkee 247667, India. [5]Centre for Environmental Sustainability and Water Security (IPASA), Research Institute for Sustainable Environment, Universiti Teknologi Malaysia, 81310 Johor Bahru, Johor, Malaysia. [6]Institute of Technology & Management, Aligarh, U.P., India.

References
Ajit K, Sarmah AK, Meyer MT, Boxall ABA. A global perspective on the use, sales, exposure pathways, occurrence, fate and effects of veterinary antibiotics (VAs) in the environment. Chemosphere. 2006;65:725–59.
Akpan UG, Hameed BH. Parameters affecting the photocatalytic degradation of dyes using TiO_2-based photocatalysts: a review. J Hazard Mater. 2009;170: 520–9.
Arslan I, Balcioglu IA, Bahnemann D. Advanced oxidation of a reactive dyebath effluent: comparison of O_3, H_2O_2/UV-C and TiO_2/UV-A processes. Water Res. 2002;36:1143–54.
Binas VD, Sambani K, Maggos T, Katsanaki A, Kiriakidis G. Synthesis and photocatalytic activity of Mn-doped TiO_2 nanostructured powders under UV and visible light. Appl Catal B: Environ. 2012;113–114:79–86.

Umar *et al. Journal of Analytical Science and Technology* (2016) 7:29

Page 8 of 8

Blake DM. Bibliography of work on the photocatalytic removal of hazardous compounds from water and air. Colorado: National Renewal Energy Laboratory; 2001.

Chaleshtori MZ, Edalatpour MHR, Masud SMS, Chianelli RR. New porous titanium–niobium oxide for photocatalytic degradation of bromocresol green dye in aqueous solution. Mater Res Bull. 2013;48:3961–7.

Chen H, Shen M, Chen R, Dai K, Peng T. Photocatalytic degradation of commercial methyl parathion in aqueous suspension containing La-doped TiO_2 nanoparticles. Environ Technol. 2011;32:1515–20.

Colon G, Maicu M, Hidalgo MC, Navıo JA. Cu-doped TiO_2 systems with improved photocatalytic activity. Appl Catal B. 2006;67:41–51.

Devi LG, Murthy N. Characterization of Mo doped TiO_2 and its enhanced photo catalytic activity under visible light. Catal Lett. 2008;125:320–30.

Devi LG, Kumar SG, Murthy BN, Kottam N. Influence of Mn^{2+} and Mo^{6+} dopants on the phase transformations of TiO_2 lattice and its photo catalytic activity under solar illumination. Catal Commun. 2009a;10:794–8.

Devi LG, Kottam N, Kumar SG. Preparation and characterization of Mn-doped titanates with a bicrystalline framework: correlation of the crystallite size with the synergistic effect on the photocatalytic activity. J Phys Chem C. 2009b; 113:15559–601.

Fan X, Chen X, Zhu S, Li Z, Yu T, Ye J, Zou Z. The structural, physical and photocatalytic properties of the mesoporous Cr-doped TiO_2. J Mol Catal A Chem. 2010;284:155–60.

Fox MA, Dulay MT. Heterogeneous photocatalysis. Chem Rev. 1993;93:341–57.

Geng J, Yang D, Zhu J, Chen D, Jiang Z. Nitrogen-doped TiO_2 nanotubes with enhanced photocatalytic activity synthesized by a facile wet chemistry method. Mater Res Bull. 2009;44:146–50.

Han C, Zhang N, Xu YJ. Structural diversity of graphene materials and their multifarious roles in heterogeneous photocatalysis. Nano Today. 2016;11:351–72.

Jin M, Nagaoka Y, Nishi K, Ogawa K, Nagahata S, Horikawa T, Katoh M, Tomida T, Hayashi J. Adsorption properties and photocatalytic activity of TiO_2 and La-doped TiO_2. Adsorption. 2008;14:257–63.

Kim SP, Choi MY, Choi HC. Photocatalytic activity of SnO_2 nanoparticles in methylene blue degradation. Mater Res Bull. 2016;74:85–9.

Knee KL, Gossett R, Boehm AB, Paytan A. Caffeine and agricultural pesticide concentrations in surface water and groundwater on the north shore of Kauai (Hawaii, USA). Mar Pollut Bull. 2010;60:1376–82.

Kolpin DW, Furlong ET, Meyer MT, Thurman EM, Zaugg SD, Barber LB, Buxton HT. Pharmaceuticals, hormones, and other organic wastewater contaminants in U.S. streams, 1999–2000: a national reconnaissance. Environ Sci Technol. 2002;36:1202–11.

Liqiang J, Xiaojun S, Baifu X, Baiqi W, Weimin C, Hongganga F. The preparation and characterization of La doped TiO_2 nanoparticles and their photocatalytic activity. J Solid State Chem. 2004;177:3375–82.

Liu B, Wang X, Cai G, Wen L, Song Y, Zhao X. Low temperature fabrication of V-doped TiO_2 nanoparticles, structure and photocatalytic studies. J Hazard Mater. 2009;169:1112–8.

Liu S, Han C, Tang ZR, Xu YJ. Heterostructured semiconductor nanowire arrays for artificial photosynthesis. Mater Horiz. 2016;3:270–82.

Lv Y, Yua L, Huang H, Liu H, Feng Y. Preparation, characterization of P-doped TiO_2 nanoparticles and their excellent photocatalystic properties under the solar light irradiation. J Alloy Comp. 2009;488:314–9.

Neppolian B, Choi HC, Sakthivel S, Arabindoo B, Murugesan V. Solar/UV-induced photocatalytic degradation of three commercial textile dyes. J Hazard Mater. 2002;89:303–17.

O¨ Kuyumcu K, Kibar E, Dayıog˘ lu K, Gedik F, Akın AN, zkara-Aydınog˘ lu O¨S. A comparative study for removal of different dyes over M/TiO_2 (M=Cu, Ni Co, Fe, Mn and Cr) photocatalysts under visible light irradiation. J Photochem Photobiol A Chem. 2015;311:176–85.

Papadimitriou VC, Stefanopoulos VG, Romanias MN, Papagiannakopoulos P, Sambani K, Tudose V, Kiriakidis G. Determination of photo-catalytic activity of un-doped and Mn-doped TiO_2 anatase powders on acetaldehyde under UV and visible light. Thin Solid Films. 2011;520:1195–201.

Paul S, Chetri P, Choudhury A. Effect of manganese doping on the optical property and photocatalytic activity of nanocrystalline titania: experimental and theoretical investigation. J Alloy Comp. 2014;583:578–86.

Peng T, Zhao D, Song H, Yan C. Preparation of lanthana-doped titania nanoparticles with anatase mesoporous walls and high photocatalytic activity. J Mol Catal A Chem. 2005;238:119–26.

Rangel-Vázquezi I, Del Angela G, Bertina V, Gonzálezb F, Vázquez-Zavalaa A, Arrietaa A, Padillac JM, Barrerad A, Ramos-Ramirezе E. Synthesis and characterization of Sn doped TiO_2 photocatalysts: effect of Sn concentration on the textural properties and on the photocatalytic degradation of 2,4-dichlorophenoxyacetic acid. J Alloy Comp. 2015;643:S144–9.

Rashad MM, Elsayed EM, Al-Kotb MS, Shalan AE. The structural, optical, magnetic and photocatalytic properties of transition metal ions doped TiO_2 nanoparticles. J Alloy Comp. 2013;581:71–8.

Raza W, Haque MM, Muneer M, Bahnemann D. Synthesis of visible light driven TiO_2 coated carbon nanospheres for degradation of dyes. 2015. http://dx.doi.org/10.1016/j.arabjc.2015.09.002.

Rovedatti MG, Castane PM, Topalian ML, Salibian A. Monitoring of organochlorine and organophosphorus pesticides in the water of the Reconquista river (Buenos Aires, Argentina). Water Res. 2001;35:3457–61.

Stengl V, Bakardjieva S. Molybdenum-doped anatase and Its extraordinary photocatalytic activity in the degradation of Orange II in the UV and vis regions. J Phys Chem C. 2010;114:19308–17.

Stengl V, Bakardjieva S, Murafa N. Preparation and photocatalytic activity of rare earth doped TiO_2 nanoparticles. Mater Chem Phys. 2009;114:217–26.

STORET water quality file. Office of water. U.S. Environmental Protection Agency data file search conducted in March. 1988.

Uhm YR, Woo SH, Kim WW, Kim SJ, Rhee CK. The characterization of magnetic and photo-catalytic properties of nanocrystalline Ni-doped TiO_2 powder synthesized by mechanical alloying. J Magn Mater. 2006;304:781–3.

Umar K, Dar AA, Haque MM, Mir NA, Muneer M. Photocatalysed decolourization of two textile dye derivatives, Martius Yellow and Acid Blue 129, in UV-irradiated aqueous suspensions of Titania, Desal. Water Treat. 2012;46:205–14.

Umar K, Haque MM, Mir NA, Muneer M. Titanium dioxide-mediated photocatalysed mineralization of two selected organic pollutants in aqueous suspensions. J Advanc Oxid Technol. 2013a;16:252–60.

Umar K, Haque MM, Muneer M, Harada T, Matsumura M. Mo, Mn and La doped TiO_2: synthesis, characterization and photocatalytic activity for the decolourization of three different chromophoric dyes. J Alloy Comp. 2013b;578:431–8.

Umar K, Aris A, Parveen T, Jaafar J, Majid ZA, Reddy AVB, Talib J. Synthesis, characterization of Mo and Mn doped Zno and their photocatalytic activity for the decolorization of two different chromophoric dyes. Appl Catal A: General. 2015;505:507–14.

Yang MQ, Xu YJ. Photocatalytic conversion of CO_2 over graphene-based composites: current status and future perspective. Nanoscale Horiz. 2016;1:270–82.

Zhang H, Zhu H. Preparation of Fe-doped TiO_2 nanoparticles immobilized on polyamide fabric. Appl Surf Sci. 2012;258:10034–41.

Zhang N, Yang MQ, Liu S, Sun Y, Xu YJ. Waltzing with the versatile platform of graphene to synthesize composite Photocatalysts. Chem Rev. 2015;115: 10307–77.

Zhu J, Chen F, Zhang J, Chen H, Anpo M. Fe^{3+}–TiO_2 photocatalysts prepared by combining sol–gel method with hydrothermal treatment and their characterization. J Photochem Photobiol A Chem. 2006;180:196–204.